南京航空航天大学

论文集

（二〇〇五年） 第33册

其他

南京航空航天大学科技部编

二〇〇六年三月

其　他

目录

序号	姓名	职称	单位	论文题目	刊物、会议名称	年、卷、期
1	胡自力 熊克 王鑫伟	副高 教授 教授	无人机院 013 013	Study on interface failure of shape memory Aiioy(SMA) reinforced smart structure with damages	Acta Mechanica sinica	20052103
2	胡自力 杨忠清	副高 副高	无人机院 无人机院	雷达罩的综合优化设计研究	宇航材料工艺	20050001
3	胡自力	副高	无人机院	Meso-mechanical analysis of shape memory alloy wires reinforced smart structures with damages	东南大学学报	20052101
4	胡自力 熊克 王鑫伟	副高 教授 教授	无人机院 013 013	SMA 增强含损伤智能结构的失效研究	复合材料学报	20050001
5	黄爱凤	初级	无人机院	翼面隐身结构电磁散射特性的数值模拟	航空学报	20052604
6	陈广东	中级	无人机院	在强杂波背景SAR图像中检测动目标	系统工程与电子技术	20052709
7	陈广东	中级	无人机院	抑制SAR图像中静止杂波背景检测慢速动目标	电子与信息学报	20052708
8	陈广东	中级	无人机院	检测 SAR 图像中径向慢速动目标	电子与信息学报	20052709
9	陈广东	中级	无人机院	测算 SAR 图像中动目标运动参数	现代雷达	20052703
10	陈广东	中级	无人机院	分数傅立叶变换用于抑制SAR杂波背景检测慢速动目标	航空学报	20052606
11	万顺生	副高	无人机院	一种翼身融合体飞行器外形的 RCS 计算与实验	南京航空航天大学学报	20053704
12	万顺生	副高	无人机院	频率选择表面天线复用副面的研究	南京航空航天大学学报	20053706
13	周欲晓	中级	无人机院	跨大气层飞行器爬升段纵向飞行控制律和制导律设计	南京航空航天大学学报	20053702
14	周欲晓	中级	无人机院	自由机翼气动特性的实验研究	实验流体力学	20051904
15	魏小龙	中级	将军路校区	基于 MSP430 的存储示波器设计	电子世界	20050004
16	魏小龙	中级	将军路校区	MSP430 串口异步通讯原理与实现	电子世界	20050003
17	魏小龙	中级	将军路校区	简单的端口、显示、中断综合应用	电子世界	20050001
18	魏小龙	中级	将军路校区	ADC12 原理与应用	电子世界	20050004
19	王小扬	副高	将军路校区	将创新教育融入电工电子实验教学的探索与实践	实验技术与管理	20052202
20	赵国安	初级	将军路校	基于 H.263 的 WEB-CAMERA 嵌入	计算机仿真	20052201

	高航	副高	区 042	式系统		
21	黄晓晴	初级	将军路校区	网络化 PXI 总线虚拟实验室设计与实现	实验室研究与探索	20052411
22	黄晓晴	初级	将军路校区	基于虚拟仪器的光学雷达监测设备的研制	测控技术	20052407
23	葛玉蓝	副高	将军路校区	开放式实验教学与工程实践能力培养	南京航空航天大学社会科学版	20050701
24	王芸	副高	将军路校区	基于 ispPAC 技术的滤波器设计	中国民航飞行学院学报	20051601
25	任为民	副高	将军路校区	小助教参与教学活动的尝试	南京航空航天大学学报(社科版)	20050701
26	黄炳辉	副高	将军路校区	学生职业生涯设计与思想政治教育的内在关系	教育评论	20050002
27	黄炳辉	副高	将军路校区	高校新校区学生思想政治工作的思考	江苏高教	20050001
28	李香莲	副高	将军路校区	汽车微弱振动信号的混沌振子识别	应用力学学报	20052204
29	李香莲 李舜酩	副高 正高	将军路校区 021	电机混沌噪声的检测	振动工程学报	200518S1
30	李香莲	副高	将军路校区	Design on automatically tracking angle system of solar energy	6th international symposium on test and measurement	2005
31	倪亚红	中级	学生处	某高校三类新生的 UPI 测评比较	中国心理卫生杂志	20051910
32	倪亚红	中级	学生处	某高校统招本科与民办本科新生 UPI 测试的对比研究	南京航空航天大学学报(社科版)	20050704
33	沈雪萍	初级	学工处	大学生职业决策困难的的测验及干预研究	第五届华人心理学家学术研讨会	2005
34	孔垂谦	副高	教务处	大学教学观念变革的实践基点	江苏高教	20050005
35	孔垂谦	副高	教务处	我国高等工程教育的“去工程化”困境与“情景化”选择	高等工程教育研究	20050001
36	王平	中级	科协	参考文献著录原则的探讨	编辑学报	20041601
37	王平	中级	科协	国内外部分科技期刊文后参考文献数量的对比分析	中国科技期刊研究	20041502
38	王平	中级	科协	国防科工委所属七所高校的学报 2003 年载文、引文的统计分析	中国科技期刊研究	20051601
39	熊春茹	正高	科协	英文版科技期刊国际化度的“国际编委比”	中国科技期刊研究	20051606
40	熊春茹	正高	科协	EI 收录科技期刊英文摘要语篇的体裁性要求	编辑学报	20051701
41	夏道家	副高	科协	大话小问题：来自编辑实践中的雏识	中国科技期刊研究	20051603

42	夏道家	副高	科协	细微加工中“改”与“不改”的尺度掌控	学报编辑论丛	20050013
43	孔令华	初级	宣传部	论媒介文化研究的两条路径	新闻与传播研究	20051201
44	孔令华	初级	宣传部	费斯克的生产性受众观	南京航空航天大学学报（人大复印资料转载）	20050701
45	田菩提	中级	机关党委	“大学生上网”负面影响分析及消解对策	南京航空航天大学学报（社科版）	20050703
46	田菩提	中级	机关党委	大学生自杀行为现象分析	江苏社会科学	20040000
47	王耘	中级	图书馆	高校图书馆阅览信息资源的聚类导读管理	图书馆论坛	20052503
48	秦萍	副高	图书馆	图书馆期刊排架方法及实践	中国图书馆学报	20050000
49	叶红	中级	图书馆	论 LCC 的编制原则及类目安排特点	南京晓庄学院学报	20052104
50	赵晨洁	中级	图书馆	人本思想在图书馆管理与服务实践中的运用	边疆经济与文化	20050003
51	赵晨洁	中级	图书馆	使用 USMARC 进行著录的若干疑问及解析	图书馆学研究	20050004
52	朱永武	中级	图书馆	隐形网站资源的获取	江西图书馆学刊	20053501
53	朱永武	中级	图书馆	基于数据挖掘的企业竞争情报系统	现代情报	20050006
54	樊泽恒	副高	高教所	基于自主学习的网络教学策略设计	中国电化教育	20050010
55	樊泽恒	副高	高教所	论高校隐/显知识转化的环境建设---知识管理视角的考察	情报科学	20052300
56	樊泽恒	副高	高教所	科技期刊数字化发展的范式转生与路径选择	中国科技期刊研究	20051601
57	李雪飞	中级	高教所	世界精神的嬗变与追求:高等教育国际化的历史思索	黑龙江高教研究	20050012
58	徐文俊	初级	高教所	浅议区域发展中非政府组织的作为	商业研究	20050005
59	郭有莘	正高	体育部	当前学校体育发展态势分析与对策	南京体育学院学报	20050005
60	吕玉军	中级	体育部	雅典奥运会中国男篮技战术指标灰色关联分析	江苏省高校第 21 届体育科学论文报告会	2005
61	郝玉 贺军萍	中级 中级	体育部	体育文化节---高校体内传统田径运动会的改革方向	山东体育科技	20052703
62	郝玉	中级	体育部	多元智能理论在体育教学设计中的应用	南京航空航天大学学报社会科学版	20050702
63	张伟	中级	体育部	普通高校体育教学改革创新问题的探讨	南京航空航天大学学报社会科学版	20050701
64	张珂	中级	体育部	优秀艺术体操运动员人格特质.运动焦虑状态对运动表现的影响	成都体育学院学报	20053104

65	苏娟	副高	体育部	谈体育课程指导纲要目标.内容的把握与实施	吉林体育学院学报	20052103
66	苏娟	副高	体育部	体育课程教学质量因素的评价与探讨	山东体育学院学报	20052103
67	王雁	中级	体育部	规则修改后艺术体操制胜因素间的关系变化及其影响	体育与科学	20052606
68	王雁	中级	体育部	王海滨在法国训练的成功启示与思考	中国体育科技	20054103
69	王雁	中级	体育部	关于普通高校健美操教学的课程及课程现代化研究	南京体育学院学报	20051906
70	王雁	中级	体育部	1994—2004 年中国击剑科研状况分析	南京体育学院学报	20050404
71	王雁	中级	体育部	王海滨备战大赛训练安排研究-----训练方法与手段选用	中国体育科学学会	2005
72	蒋晔	中级	体育部	对高校女生排球选项课实施教学和考评相结合效果分析	南京体育学院学报	20051906
73	蒋晔	中级	体育部	不同气压.不同风速及对称性对排球飘球的影响	中国体育科技	20054105
74	蒋晔	中级	体育部	中国女排在世界杯和奥运会比赛中发球技术的分析研究	南京体育学院学报	20050403
75	蒋晔	中级	体育部	不同风速及对称性对排球飘晃距离的影响	武汉体育学院学报	20053911
76	杜长亮	初级	体育部	“网球肘”的成因、预防与治疗	吉林体育学院学报	20052101
77	郭洪波	中级	体育部	运用血乳酸对我国优秀激流回旋运动员训练强度的研究	山东体育学院学报	20050202
78	郭洪波	中级	体育部	甘肃省青少年男子短跑运动员体型分析	西北师范大学学报	20054103
79	蒋诗泉	中级	体育部	发达国家社会体育发展经费募集的社会化运作研究	南京体育学院学报	20051905
80	蒋诗泉	中级	体育部	江苏省中小学生 1990—2004 年体质健康调查分析	吉林体育学院学报	20052103
81	蒋诗泉	中级	体育部	社会转型时期高校体育教师的心理困惑与思考	中华创新教育	20050007
82	蒋诗泉	中级	体育部	体育教师非言语评价的因素分析	中国教育教学杂志	200517114
83	马彬	初级	体育部	对我国体育院校篮球专项学生裁判能力培养优势的调查与研究	南京体育学院学报	20050402
84	顾若兵	中级	体育部	太极拳锻炼对中老年人细胞代谢功能的影响	贵州体育科技	20050004
85	翟元	初级	体育部	确立“健康第一”思想，培养终身体育习惯	南航体育科技会	2005
86	陈华卫	初级	体育部	美国爱达荷州健康教师标准研究	体育文化导刊	20050005

87	陈华卫	初级	体育部	中学体育与健康课程内容标准实施现状的调查研究	第三届中国学校体育科学大会	2005
88	杨峰	中级	体育部	大学体育与健康课程教学新视野研究性学习	南京体育学院学报	20051905
89	杨峰 翟元	中级 初级	体育部	箭步抓举训练对少年女排运动员弹跳能力的影响	吉林体育学院学报	20052101
90	杨峰	中级	体育部	对优秀女运动员大强度训练期体内微量元素的运动变化研究	四川体育科学	20050003
91	杨峰 翟元	中级 初级	体育部	有氧耐力运动对小鼠肌肉组织自由基损伤的影响	武汉体育学院学报	20053906
92	陈建杰	中级	体育部	普通高校体育理论课网络辅助教学模式初探	江苏省高校第21届体育科学论文报告会	2005
93	陈建杰	中级	体育部	中国排球运动可持续发展浅谈	南京航空航天大学学报社科版	20050702
94	陈建杰	中级	体育部	多媒体技术在体育理论教学中的应用	泰安教育学院学报岱宗学刊	20050004
95	吕常魁	中级	工程训练中心	一种新的运动检测及轮廓追踪方法	武汉大学学报(信息科学版)	20053008
96	王姝歆	中级	工程训练中心	复合型柔性铰链机构特性及其应用研究	光学精密工程	20051305
97	王姝歆	中级	工程训练中心	微型仿生扑翼飞行器的尺度效应分析	南京航空航天大学学报	20053706
98	王姝歆	中级	工程训练中心	复合型柔性铰链的折叠成型技术研究	机械制造	20050012
99	谭白磊	中级	后勤管理处	对当前房地产泡沫经济问题的思考	集团经济研究	20050178
100	谭白磊	中级	后勤管理处	高校后勤服务市场化改革之我见	集团经济研究	20050184
101	张继斌		后勤管理处	浅析高校节能管理	高校后勤研究	20050005
102	许琴	副高	发展规划处	从统计角度看国内大学排名	统计与决策	20050002
103	程永波	中级	学科办	Research on the scientific and technological innovation of research university and its measures	US-China Education Review	20050203
104	陈旭	副高	教务处	建立新的机制,实现产学研合作的可持续发展	中国大学教学	20050003
105	陈旭	副高	教务处	数字化校园建设需要技术与文化的协调	江苏教育学院学报	20052102
106	陈旭	副高	教务处	面向国际竞争的航空航天专业教学改革研究与探索	南京航空航天大学学报社科版	20050701
107	陈旭	副高	教务处	现代质量观下的工科基础课程教学	电气电子教学学	20050027

				基地建设	报	
108	陈旭	副高	教务处	New courses in engineering education programmes in NUAA	The Twelfth international conference on learning	2005
109	郑立宇	中级	后勤	高校师生员工参与型后勤管理模式初探	中国高等教育	20050006
110	刘建成	中级	学生处	大学生思想政治教育有效途径的探索与实践	教育与职业	20050035
111	刘建成	中级	学生处	大学生学风状况调查及加强学风建设的对策思考	南京航空航天大学学报社科版	20050702
112	张迎春	初级	学生处	价值包和顾客价值研究及其在旅行社行业的应用	市场周刊.研究版	2005.10

Acta Mech Sinica (2005) 21, 286–293
DOI 10.1007/s10409-005-0031-0

RESEARCH PAPER

Zili Hu · Ke Xiong · Xinwei Wang

Study on interface failure of shape memory alloy (SMA) reinforced smart structure with damages*

Received: 4 March 2004 / Revised: 18 November 2004 / Accepted: 25 November 2004 / Published online: 31 May 2005

Abstract Shape memory alloy (SMA) reinforced smart structure can be used to make structural shape and strength self-adapted and structural damage self-restrained. Although SMA smart structures without damages were extensively studied, researches on SMA smart structures with damages have rarely been reported thus far. In this paper, thermo-mechanical behaviors of SMA fiber reinforced smart structures with damages are analyzed through a shear lag model and the variational principle. Mathematical expressions of the meso-displacement field and the stress-strain field of a typical element with damages are obtained, and a failure criterion for interface failure between SMA fibers and matrix is established, which is applied to an example. Results presented herein may provide a theoretical foundation for further studies on integrity of SMA smart structures.

Keywords Smart structures · Damages · SMA · Failure · Meso-mechanics analysis · Variational principle

1 Introduction

Smart structures have attracted more and more attention due to their dual properties of conventional composite structures and of functional composite structures. They are being applied in fields such as aeronautics & astronautics, national defense, architecture, medicine [1–4]. Among them, the shape memory alloy (SMA) reinforced smart structure could be used to make the structural shape and strength self-adaptive and to prevent structure failures. Although SMA smart structures without damages were extensively studied [5–10], researches on SMA smart structures with damages have rarely reported thus far [11,12]. In this paper, thermo-mechanical behaviors of SMA fiber reinforced smart structures with damages are analyzed by utilizing a shear lag model and the variational principle. Mathematical expressions of the meso-displacement field and the stress-strain field of a typical element with damages are obtained, and a failure criterion for interface failure between SMA wires and matrix is established, which is applied to an example. Results presented herein may provide a theoretical basis for further studies on integrity of SMA smart structures.

* The project supported by the National Natural Science Foundation of China (10072026, 50135030) and Aeronautical Science Foundation of China (01G52041)
The English text was polished by Keren Wang.

Z. L. Hu(✉) · K. Xiong · X. W. Wang
The Aeronautical Science Key Laboratory for Smart Materials and Structures, Nanjing University of Aeronautics and Astronautics, Nanjing 210016, China
E-mail: huzlgp@163.com
Tel: 086-025-84892860

2 Stress field of SMA reinforced smart structure

In an SMA reinforced smart structure, both the stress distribution in SMA and the interaction between SMA fibers and matrix are very complicated, because they are related not only to the shape memory effect, bonding interfaces and boundary conditions, but also to damages of interfaces. Therefore a simplified mechanical model, a shear lag model, is applied in the following analysis, assuming that fibers are only subjected to an axial pulling load, and the matrix and interfaces are only subjected to shearing load [13].

Considering a typical element of the SMA reinforced smart structure as shown in Fig. 1, applying the shear lag model to the element, a balance equation of force can be obtained as

$$\pi r^2\sigma_f + 2\pi r_f\tau_i \mathrm{d}z = \pi r^2(\sigma_f + \mathrm{d}\sigma_f), \tag{1}$$

which can be rewritten into

$$\frac{\mathrm{d}\sigma_f}{\mathrm{d}z} = \frac{2\tau_i}{r_f}, \tag{2}$$

where σ_f is the axial stress in the SMA fiber, τ_i is the shear stress on interface, r_f is the radius of the SMA fiber.

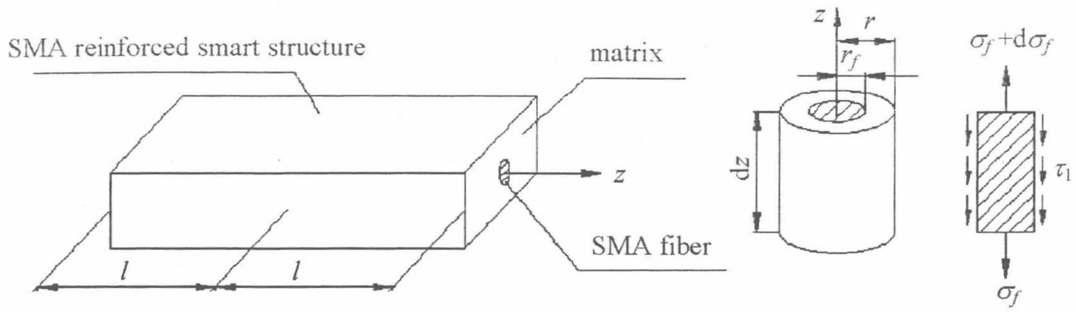

Fig. 1 Typical element of SMA reinforced smart structure

2.1 One-dimensional constitutive relation of SMA

In this paper, Tanaka model is applied as one-dimensional constitutive relation for SMA, that is,

$$\sigma - \sigma_0 = D(\varepsilon - \varepsilon_0) + \Omega(\xi - \xi_0) + \Theta(T - T_0), \tag{3}$$

where the converse martensitic transformation kinetics model is

$$(M \to A) \quad \xi = \frac{\xi_M}{A_s - A_f}\Big(T - A_f - \frac{\sigma}{C_A}\Big). \tag{4}$$

Equation (3) is applied in three different stages as follows: In the first stage (before the converse transformation):

$$\sigma - \sigma_0 = D(\varepsilon - \varepsilon_{res}) + \Theta(T - T_0). \tag{5}$$

In the second stage (in the converse transformation):

$$\Big[1 - \frac{\Omega\xi_M}{(A_f - A_s)C_A}\Big]\sigma - \sigma_{A_s^\sigma} = D(\varepsilon - \varepsilon_{A_s^\sigma}) + \Theta(T - A_s^\sigma) + \Omega\xi_M\Big(\frac{A_f - T}{A_f - A_s} - 1\Big). \tag{6}$$

In the third stage (after the converse transformation):

$$\sigma - \sigma_{A_f^\sigma} = D(\varepsilon - \varepsilon_{A_f^\sigma}) + \Theta(T - A_f^\sigma), \tag{7}$$

where $\varepsilon_{A_s^\sigma}$, $\sigma_{A_s^\sigma}$ and $\varepsilon_{A_f^\sigma}$, $\sigma_{A_f^\sigma}$ are the strain and the stress corresponding to A_s^σ and A_f^σ, respectively.

SMA should be stretched before embedded into matrix, and fixed at the ends to be prevented from shrinking, thus, the initial strain of Eq. (3) is just the pre-strain of SMA before solidifying of matrix, that is, $\varepsilon_0 = \varepsilon_{res}$.

For convenience, Eqs. (5)–(7) are written into a uniform form as

$$\varepsilon^r = \varepsilon - \varepsilon_{res} = k_1\sigma + k_2, \tag{8}$$

where ε^r, ε and ε_{res} are the restoring strain, total strain and pre-strain, respectively, k_1 and k_2 are the effective restoring flexibility and effective free restoring strain, respectively, which are expressed as follows:

Before the converse transformation

$$k_1 = \frac{1}{D}, k_2 = -\frac{\Theta}{D}(T - T_0). \tag{9}$$

In the converse transformation

$$k_1 = \Big[1 - \frac{\Omega\xi_M}{(A_f - A_s)C_A}\Big]\Big/D,$$
$$k_2 = (\varepsilon_{A_s^\sigma} - \varepsilon_{res}) + \Big[\Theta A_s^\sigma - \Big(\Theta - \frac{\Omega\xi_M}{A_f - A_s}\Big)T - \frac{\Omega\xi_M}{A_f - A_s}A_s - \sigma_{A_s^\sigma}\Big]\Big/D. \tag{10}$$

After the converse transformation

$$k_1 = \frac{1}{D},$$
$$k_2 = (\varepsilon_{A_f^\sigma} - \varepsilon_{res}) + [\Theta(A_f^\sigma - T) - \sigma_{A_f^\sigma}]/D. \tag{11}$$

2.2 Linear elasticity hypothesis of shear deformation on interface

Assume that the relation between shear strain and shear stress on interface follows the linear elasticity hypothesis. To obtain the shear strain and shear stress on interface, the shear strain and shear stress in the matrix should be determined first. Assuming that $w(r, z)$ is the axial displacement of any point in the matrix, and ignoring the variation of the radial displacement over axial coordinate z, according to Hook's law, the corresponding shear stress can be expressed as

$$\tau = G_m\frac{\partial w}{\partial r}, \tag{12}$$

where G_m is the shear modulus of the matrix.

Considering force balance of any cylinder in the matrix, we obtain

$$2\pi r_f\tau_i = 2\pi r\tau. \tag{13}$$

Substituting Eq. (12) into Eq. (13) and integrating

$$\int_{w_f}^{w_R}\partial w = \frac{r_f\tau_i}{G_m}\int_{r_f}^{R}\frac{\partial r}{r}, \tag{14}$$

we obtain

$$\tau_i = \frac{G_m(w_R - w_f)}{r_f\ln(R/r_f)}, \tag{15}$$

where w_f is the axial displacement of the SMA fiber at $r = r_f$, w_R is the axial displacement in the matrix at $r = R$, and

$$\frac{\partial w_R}{\partial z} = \varepsilon_0, \tag{16}$$

where ε_0 is the axial strain in the matrix at $r = R$, which is defined as the average strain of the SMA reinforced smart structure. Substituting Eq. (15) into Eq. (2), one obtains

$$\frac{d\sigma_f}{dz} = -\frac{2G_m(w_R - w_f)}{r_f^2 \ln(R/r_f)}. \tag{17}$$

Taking derivative of Eq. (17) with respect to z and noting that

$$\frac{dw_f}{dz} = \varepsilon_f = \varepsilon^r, \tag{18}$$

and Eq. (8), we have

$$\frac{d^2\sigma_f}{dz^2} = -\frac{2G_m}{r_f^2 \ln(R/r_f)}(\varepsilon_0 - k_2 - k_1\sigma_f). \tag{19}$$

Let $n^2 = \dfrac{2G_m k_1}{r_f^2 \ln(R/r_f)}$, then Eq. (19) can be rewritten into

$$\frac{d^2\sigma_f}{dz^2} = n^2\Big(\sigma_f - \frac{\varepsilon_0 - k_2}{k_1}\Big). \tag{20}$$

The solution of Eq. (20) can be expressed as

$$\sigma_f = \frac{\varepsilon_0 - k_2}{k_1} + B\sinh(nz) + D\cosh(nz), \tag{21}$$

where k_1 and k_2 are related to the converse transformation process. As a result of k_2 depending on temperature parameter T, Eq. (21) gives the axial stress distribution in the SMA fiber at different temperatures. The importance of Eq. (21) rests with the fact that the stress distribution of smart structures can be regulated by controlling the temperature variation of SMA fibers which are embedded in smart structures to make the structural shape and strength self-adapted and the structural damage self-restrained, as shown in Fig. 2.

In Eq. (21), B and D are determined by boundary conditions of SMA fibers. If the length of SMA fibers is $2l$, its midpoint is the center of the coordinate, the boundary conditions can be considered in three cases: (1) $\sigma_f = 0$ at $z = \pm l$ (ends free); (2) $\sigma_f = -k_2/k_1$ at $z = \pm l$ (ends fixed); (3) $\sigma_f = \sigma_f^0$ at $z = \pm l$(σ_f^0 is the dead external stress at the ends). As an example, in the first case, we obtain

$$B = 0, \quad D = -\frac{\varepsilon_0 - k_2}{k_1\cosh(nl)}.$$

Then, the axial stress of SMA fiber is expressed as

$$\sigma_f = \frac{\varepsilon_0 - k_2}{k_1}\Big[1 - \frac{\cosh(nz)}{\cosh(nl)}\Big]. \tag{22}$$

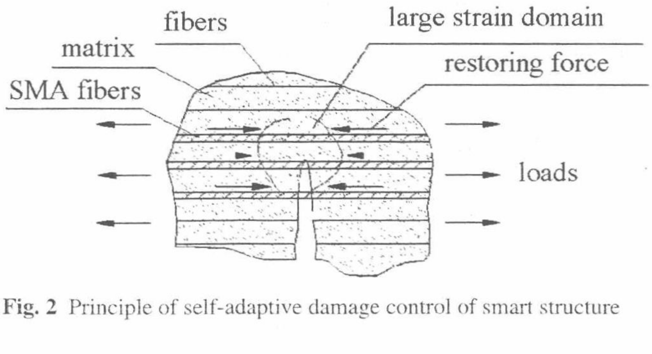

Fig. 2 Principle of self-adaptive damage control of smart structure

Substituting Eq. (22) into Eq. (2), the shear stress of interface can be obtained as

$$\tau_i = -\frac{nr_f(\varepsilon_0 - k_2)}{2k_1\cosh(nl)}\sinh(nz). \tag{23}$$

It is known by Eqs. (22) and (23) that the maximum shear stress of interface occurs at the ends ($z = \pm l$) of SMA fiber in the converse directions, but the maximum axial pulling stress occurs at the midpoint ($z = 0$) of SMA fiber. The same is true of other two cases.

Above analysis results show that the strength of a smart structure can be self-adaptively controlled by SMA fibers embedded in the smart structure. But one should also be wary of a new kind of failure: when the maximum shear stress $\tau_{i\,\max}$ of interface at ends of SMA fibers is equal to the shear strength τ_b, the initial failures may occur at the ends.

3 Failure analysis of SMA reinforced smart structures with damages

There are three restoring states of SMA in smart structures: the free restoring state, the restrained restoring state and the controlled restoring state. Consider the controlled restoring state, which is near to the actual situation.

3.1 Analysis model and typical element

Assume that the analysis object is an SMA reinforced one-directional composite, with partial failures of interface at the ends, but still with bridge and friction effects between peeled faces, resisting further peeling damage development. We use the equivalent friction shear stress τ_p to denote the degree of resistance effect, and assume that

$$\tau_p = \tau_0\frac{l}{L}, \tag{24}$$

where τ_0 denotes the instantaneous equivalent friction shear stress just after initial peeling, and $0 \le \tau_0 \le \tau_b$ (when $l = L$, $\tau_0 = \tau_b$), τ_b is the shear yield strength of the interface.

A typical element of the SMA reinforced smart structure with damages is shown in Fig. 3, where L is half length of the element, l is the length of a portion without damage, $L - l$ is the length of a peeled portion, r_f is the radius of SMA fiber, r is the radius of any cylinder in the matrix. Let R denote the radius of the maximum cylinder in matrix, and we still define ε_0 as average strain of the SMA reinforced smart structure, then, we can obtain $w_R = \varepsilon_0 z$ by Eq. (16) and the boundary condition ($z = 0$, $w_R = 0$). P_a is a concentrated load at ends of SMA fiber, and we have $P_a = \pi r_f^2\sigma_a$, in which σ_a is the average stress at ends of SMA fiber.

3.2 Variational principle on failure of SMA reinforced smart structure with damages

We consider only a half of the typical element because of symmetry, the strain energy u^e of the typical element is com-

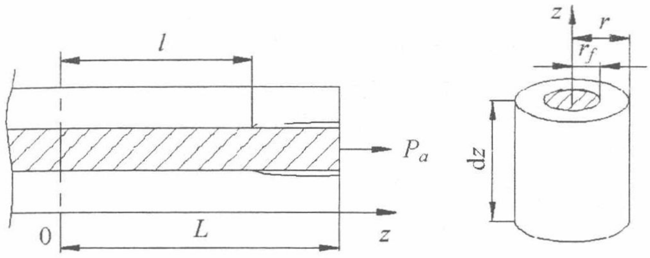

Fig. 3 Typical element of SMA reinforced smart structure with damages

posed of the tensile strain energy u^f of SMA fiber and the shearing strain energy u^m of matrix. Therefore, we have

$$u^e = u^f + u^m, \tag{25}$$

where

$$u^f = \int_V \frac{1}{2}\sigma_f \varepsilon_f \mathrm{d}V, \tag{26}$$

$$\begin{aligned} u^m &= \frac{1}{2G_m}\int_V \tau^2 \mathrm{d}V \\ &= \frac{1}{2G_m}\int_0^l \int_0^{2\pi}\int_{r_f}^R \left(\frac{r_f}{r}\tau_i\right)^2 r\mathrm{d}r\mathrm{d}\theta\mathrm{d}z \\ &\quad + \frac{1}{2G_m}\int_l^L \int_0^{2\pi}\int_{r_f}^R \left(\frac{r_f}{r}\tau_p\right)^2 r\mathrm{d}r\mathrm{d}\theta\mathrm{d}z \\ &= \frac{\pi r_f^2 \ln(R/r_f)}{G_m}\int_0^l \tau_i^2 \mathrm{d}z + \frac{\pi r_f^2 \ln(R/r_f)}{G_m}\int_l^L \tau_p^2 \mathrm{d}z. \end{aligned} \tag{27}$$

Substituting Eq. (8) and Eq. (18) into Eq. (26), we obtain

$$u^f = \frac{\pi r_f^2}{2k_1}\int_0^L \left[\left(\frac{\mathrm{d}w_f}{\mathrm{d}z}\right)^2 - k_2\frac{\mathrm{d}w_f}{\mathrm{d}z}\right]\mathrm{d}z. \tag{28}$$

Substituting Eq. (15) into Eq. (27), we have

$$\begin{aligned} u^m &= \frac{\pi G_m}{\ln(R/r_f)}\int_0^l (w_R - w_f)^2 \mathrm{d}z \\ &\quad + \frac{\pi r_f^2 \ln(R/r_f)}{G_m}\tau_p^2 (L-l). \end{aligned} \tag{29}$$

Thus, the functional of the potential energy can be expressed as

$$\Pi^e = 2\left(u^f + u^m - P_a w_f(L) + \int_l^L f_p w_f \mathrm{d}z\right), \tag{30}$$

where f_p is the equivalent friction shear stress of the peeled portion in a unit of length, and $f_p = 2\pi r_f \tau_p$.

According to the principle of the minimum potential energy [14,15], the first variation of the functional of the potential energy is equal to zero, that is,

$$\delta\Pi^e[w_f(z)] = 0. \tag{31}$$

Then, we obtain

$$\begin{aligned} &\frac{\pi r_f^2}{2k_1}\int_0^L \left(2\frac{\mathrm{d}w_f}{\mathrm{d}z}\frac{\mathrm{d}\delta w_f}{\mathrm{d}z} - k_2\frac{\mathrm{d}\delta w_f}{\mathrm{d}z}\right)\mathrm{d}z \\ &+ \frac{\pi G_m}{\ln(R/r_f)}\int_0^l 2(w_R - w_f)(\delta w_R - \delta w_f)\mathrm{d}z \\ &- P_a \delta w_f\big|_L + \int_l^L f_p \delta w_f \mathrm{d}z = 0. \end{aligned} \tag{32}$$

Integrating the first term of the above equation, and noting that $\delta w_R = 0$ (where w_R is defined as the known displacement), we have

$$\begin{aligned} &\frac{\pi r_f^2}{k_1}\left(\frac{\mathrm{d}w_f}{\mathrm{d}z}\delta w_f\Big|_0^L - \int_0^L \delta w_f \frac{\mathrm{d}^2 w_f}{\mathrm{d}z^2}\mathrm{d}z\right) - \frac{k_2 \pi r_f^2}{2k_1}\delta w_f\Big|_0^L \\ &+ \frac{\pi G_m}{\ln(R/r_f)}\int_0^l 2(w_R - w_f)(-\delta w_f)\mathrm{d}z \\ &- P_a \delta w_f\big|_L + \int_l^L f_p \delta w_f \mathrm{d}z = 0. \end{aligned} \tag{33}$$

Because $\delta w_f(0) = 0$, Eq. (33) can be rewritten as

$$\begin{aligned} &\left(\frac{\pi r_f^2}{k_1}\frac{\mathrm{d}w_f}{\mathrm{d}z}\Big|_L - \frac{k_2 \pi r_f^2}{2k_1} - P_a\right)\delta w_f\big|_L \\ &- \frac{\pi r_f^2}{k_1}\int_0^L \frac{\mathrm{d}^2 w_f}{\mathrm{d}z^2}\delta w_f \mathrm{d}z \\ &- \frac{2\pi G_m}{\ln(R/r_f)}\int_0^l (w_R - w_f)\delta w_f \mathrm{d}z \\ &+ \int_l^L f_p \delta w_f \mathrm{d}z = 0. \end{aligned} \tag{34}$$

Now introduce the function

$$\langle z - l\rangle = \begin{cases} 1, & 0 \le z \le l, \\ 0, & l < z \le L. \end{cases} \tag{35}$$

The domain of definition of the function is [0, L].

Thus, Eq. (34) becomes

$$\begin{aligned} &\left(\frac{\pi r_f^2}{k_1}\frac{\mathrm{d}w_f}{\mathrm{d}z}\Big|_L - \frac{k_2 \pi r_f^2}{2k_1} - P_a\right)\delta w_f\big|_L \\ &- \frac{\pi r_f^2}{k_1}\int_0^L \frac{\mathrm{d}^2 w_f}{\mathrm{d}z^2}\delta w_f \mathrm{d}z \\ &- \frac{2\pi G_m}{\ln(R/r_f)}\int_0^L (w_R - w_f)\langle z - l\rangle \delta w_f \mathrm{d}z \\ &+ \int_0^L f_p (1 - \langle z - l\rangle)\delta w_f \mathrm{d}z = 0. \end{aligned} \tag{36}$$

To any small virtual displacement, the first term of the above equation gives the boundary condition

$$\frac{\pi r_f^2}{k_1}\frac{\mathrm{d}w_f}{\mathrm{d}z}\Big|_L - \frac{k_2 \pi r_f^2}{2k_1} - P_a = 0. \tag{37}$$

And other terms give the governing equation

$$\begin{aligned} &-\frac{\pi r_f^2}{k_1}\frac{\mathrm{d}^2 w_f}{\mathrm{d}z^2} - \frac{2\pi G_m}{\ln(R/r_f)}(w_R - w_f)\langle z - l\rangle \\ &+ f_p (1 - \langle z - l\rangle) = 0. \end{aligned} \tag{38}$$

Expressing Eq. (38) in different portions and solving it, we have in the portion $0 \le z \le l$,

$$-\frac{\pi r_f^2}{k_1}\frac{d^2 w_f}{dz^2} - \frac{2\pi G_m}{\ln(R/r_f)}(w_R - w_f) = 0. \quad (39)$$

Let $n^2 = \frac{2k_1 G_m}{r_f^2 \ln(R/r_f)}$, and note that $w_R = \varepsilon_0 z$, then the above equation can be written as

$$\frac{d^2 w_f}{dz^2} + n^2(\varepsilon_0 z - w_f) = 0. \quad (40)$$

Differentiating Eq. (40) with respect to z, and let $y = \frac{dw_f}{dz}$, we have

$$\frac{d^2 y}{dz^2} - n^2 y = -n^2 \varepsilon_0. \quad (41)$$

The solution of Eq. (41) is

$$y = C_1 \sinh(nz) + C_2 \cosh(nz) + \varepsilon_0. \quad (42)$$

Therefore,

$$w_f(z) = \frac{C_1}{n}\cosh(nz) + \frac{C_2}{n}\sinh(nz) + \varepsilon_0 z + C_3, \quad (43)$$

where C_1, C_2 and C_3 are coefficients to be determined.

In the portion $l < z \le L$, we have

$$-\frac{\pi r_f^2}{k_1}\frac{d^2 w_f^p}{dz^2} + f_p = 0, \quad (44)$$

where w_f^p denotes the displacement of SMA fiber in the peeled portion. The solution of Eq. (44) is

$$w_f^p = \frac{k_1 \tau_p}{r_f} z^2 + C_4 z + C_5, \quad (45)$$

where C_4 and C_5 are coefficients to be determined. In addition to the boundary condition expressed as Eq. (37), there are other four boundary conditions as follows

$$w_f\big|_0 = 0, \quad (46)$$

$$w_f\big|_l = w_f^p\big|_l, \quad (47)$$

$$\frac{dw_f}{dz}\Big|_l = \frac{dw_f^p}{dz}\Big|_l, \quad (48)$$

$$\tau_p = \frac{G_m(w_R - w_f^p)}{r_f \ln(R/r_f)}, \quad (49)$$

where $w_R = \varepsilon_0 z$. Therefore, we can establish equations for the coefficients through Eqs. (37) and (45)–(49)

$$\begin{aligned}
&\frac{C_1}{n} + C_3 = 0,\\
&C_1 \sinh(nl) + C_2 \cosh(nl) + \varepsilon_0 = \frac{2k_1 \tau_p l}{r_f} + C_4,\\
&\frac{C_1}{n}\cosh(nl) + \frac{C_2}{n}\sinh(nl) + \varepsilon_0 l + C_3\\
&\quad = \frac{k_1 \tau_p}{r_f} l^2 + C_4 l + C_5,\\
&\frac{\pi r_f^2}{k_1}\left(\frac{2k_1 \tau_p}{r_f} L + C_4\right) - \frac{k_2 \pi r_f^2}{2k_1} - P_a = 0,\\
&\varepsilon_0 z\big|_L - \frac{\tau_p r_f \ln(R/r_f)}{G_m} = \frac{k_1 \tau_p}{r_f} z^2\big|_L + C_4 z\big|_L + C_5.
\end{aligned} \quad (50)$$

The solutions of above equations are

$$C_4 = \frac{k_2}{2} + \sigma_a k_1 - \frac{2k_1 \tau_0 l}{r_f}, \quad (51)$$

$$C_5 = \left(\varepsilon_0 - \frac{k_2}{2} - \sigma_a k_1\right)L - \frac{\tau_0 l r_f \ln(R/r_f)}{G_m L} + \frac{k_1 \tau_0 L l}{r_f}, \quad (52)$$

$$\begin{aligned}
C_1 = &\frac{\varepsilon_0 \sinh(nl) - n\varepsilon_0 l \cosh(nl)}{1 - \cosh(nl)}\\
&+ \frac{k_1 \tau_0 l^2 [nl \cosh(nl) - 2\sinh(nl)]}{[1 - \cosh(nl)] L r_f}\\
&+ \frac{nl \cosh(nl) - \sinh(nl)}{1 - \cosh(nl)} C_4 + \frac{n \cosh(nl)}{1 - \cosh(nl)} C_5,
\end{aligned} \quad (53)$$

$$\begin{aligned}
C_2 = &\frac{2k_1 \tau_0 l^2}{L r_f \cosh(nl)} + \frac{C_4}{\cosh(nl)}\\
&- \frac{\varepsilon_0}{\cosh(nl)} - \frac{C_1 \sinh(nl)}{\cosh(nl)},
\end{aligned} \quad (54)$$

$$C_3 = -\frac{C_1}{n}. \quad (55)$$

In the portion $0 \le z \le l$, we can solve for the shear stress of interface between SMA fiber and matrix via the shear lag model.

$$\tau_i = \frac{G_m(w_R - w_f)}{r_f \ln(R/r_f)}. \quad (56)$$

Substituting Eq. (43) into Eq. (56), we have

$$\tau_i = \frac{G_m\left[-\frac{C_1}{n}\cosh(nz) - \frac{C_2}{n}\sinh(nz) - C_3\right]}{r_f \ln(R/r_f)}. \quad (57)$$

Thus, the maximum shear stress of the interface can be obtained at point $z = l$

$$\tau_{i\,\max} = \frac{G_m\left[-\frac{C_1}{n}\cosh(nl) - \frac{C_2}{n}\sinh(nl) - C_3\right]}{r_f \ln(R/r_f)}. \quad (58)$$

In the portion $l < z \leq L$, a testing analysis is undertaken via the shear lag model. From the following relations

$$\varepsilon_f^p = \frac{\mathrm{d}w_f^p}{\mathrm{d}z}, \tag{59}$$

$$\sigma_f^p = \frac{1}{k_1}(\varepsilon_f^p - k_2), \tag{60}$$

$$\tau_i = \frac{r_f}{2}\frac{\mathrm{d}\sigma_f^p}{\mathrm{d}z}. \tag{61}$$

We obtain

$$\tau_i = \tau_p. \tag{62}$$

This result is completely in agreement with the initial assumption about the equivalent friction shear stress, therefore, it also provides a proof that the variational method of the issue is correct. Through the above analysis, we can obtain the distribution of the interface shear stress τ_i as shown in Fig. 4.

3.3 A criterion of interface failure for SMA reinforced smart structure with damage

Substituting C_1, C_2 and C_3 into Eq. (58), we finally obtain

$$\tau_{i\,\max} = \frac{k_1 G_m (L-l)}{r_f \ln(R/r_f)}\left[\sigma_a - \frac{\tau_0 l(L-l)}{L r_f} - \frac{\varepsilon_0}{k_1} + \frac{k_2}{2k_1}\right] + \frac{\tau_0 l}{L}. \tag{63}$$

When $\tau_{i\,\max}$ reaches the shear strength τ_b of interface, the interface failure takes place. Therefore, a criterion of interface failure for SMA reinforced smart structure with damages can be established as

$$\tau_{i\,\max} \leq \tau_b. \tag{64}$$

Equation (63) actually contains two kinds of actuation: dead-load and temperature. The temperature is reflected in parameter k_2. It is not difficult to see that there are many factors in a failure criterion for interface failure, including interface properties, dead-load, temperature, thermodynamical properties of SMA, initial debonding length $L - l$.

Let $\tau_{i\,\max} = \tau_b$, then the stress σ_a is defined as the debonding stress, and denoted by σ_a^T

$$\sigma_a^T = \frac{r_f \ln(R/r_f)(\tau_b L - \tau_0 l)}{k_1 G_m L(L-l)} + \frac{\tau_0 l(L-l)}{L r_f} + \frac{\varepsilon_0}{k_1} - \frac{k_2}{2k_1}. \tag{65}$$

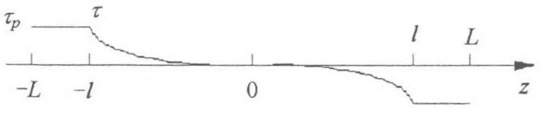

Fig. 4 The distribution of the interface shear stress τ_i of typical element of SMA reinforced smart structure with damages

3.4 An example

Considering three cases for the sake of comparing with each other.

(1) case 1: Taking NiTi fiber reinforced composite for an example, the composite modulus of the material in the tensile direction is $E_C = 6.82\,\mathrm{GPa}$ ($E_C = E_a V_a + E_m V_m$), and the shear modulus of matrix is $G_m = 2.94\,\mathrm{GPa}$. The NiTi fiber's residual deformation in martensitic is 3%, that is, $\varepsilon_{res} = 3\%$, its radius is $r_f = 0.75\,\mathrm{mm}$, its volume percentage is $V_a = 10\%$, and other parameters of the material are listed in Table 1. Let $L = 250\,\mathrm{mm}$, $l = 200\,\mathrm{mm}$, and $R/r_f = 3$. τ_b and τ_0 are determined from experiment [12–16] as shown in Table 2;

(2) case 2: $\varepsilon_{res} = 2\%$, $V_a = 10\%$, and other parameters are the same as those of case 1;

(3) case 3: $\varepsilon_{res} = 3\%$, $V_a = 20\%$, and other parameters are the same as those of case 1.

Suppose that NiTi fiber reinforced composites is orthotropic, ignoring the Poisson effect resulted from transverse strain, we obtain

$$\varepsilon_0 = \frac{\sigma_C}{E_C} = \left(\frac{r_f}{R}\right)^2 \frac{\sigma_a^T}{E_C}, \tag{66}$$

where $\pi r_f^2 \sigma_a^T = \pi R^2 \sigma_C$ by the shear lag model.

Substituting the above equation into Eq. (65), we have

$$\sigma_a^T = \frac{R^2 E_C k_1}{R^2 E_C k_1 - r_f^2}\left[\frac{r_f \ln(R/r_f)(\tau_b L - \tau_0 l)}{k_1 G_m L(L-l)} + \frac{\tau_0 l(L-l)}{L r_f} - \frac{k_2}{2k_1}\right]. \tag{67}$$

To different actuating temperatures, k_1 and k_2 should be calculated in the corresponding transformation stage, where $\sigma_{A_s^\sigma}$ is determined by Eq. (5) corresponding to the end of the first stage and $\sigma_{A_f^\sigma}$ is determined by Eq. (6) corresponding to the end of the second stage. Furthermore, it is known by the constraining condition of the interface that $\varepsilon_{A_s^\sigma} = \varepsilon_0$ in the second stage and $\varepsilon_{A_f^\sigma} = \varepsilon_0$ in the third stage.

A numerical result is shown in Fig. 5. In Fig. 5(a), if a point M with two kinds of actuation (dead-load and temperature) is in the shadow domain, the interface failure will not

Table 1 Material parameters of Ni-49.2% at Ti fiber

D (MPa)	Ω	Θ (MPa/°C)	M_f	M_s	A_s (°C)	A_f	C_A	C_M (MPa/°C)
1.8×10^4	−489.8	−0.4	−3	2	45	63	14.8	14.8

Table 2 Experimental value of τ_b and τ_0

Transformation state	τ_b/(N·mm^2)	τ_0/(N·mm^2)
before converse transformation	0.96	0.72
in converse transformation	0.86	0.65
after converse transformation	0.75	0.56

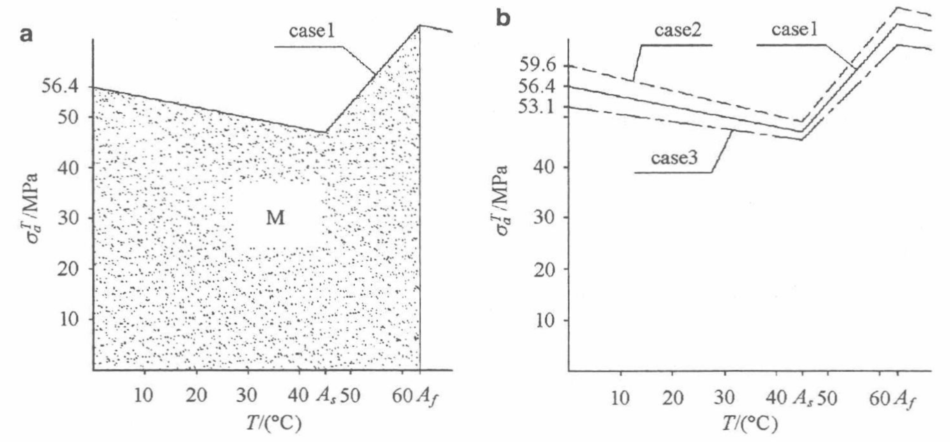

Fig. 5 Numerical result of the interface failure

occur; if the point is on the boundary of the shadow domain, the interface yielding begins; if the point is out of the shadow domain, the SMA reinforced smart structures will fail in self-adaptation. In the temperature domain of $A_s \leq T \leq A_f$, the failure boundary turns with a considerable slope upward since SMA fiber is in the temperature actuating state. In the temperature domain $T_0 \leq T \leq A_s$ and $T \geq A_f$, the failure boundary declines since the matrixes soften with temperature ascending. In the above example, $A_f = 63°\mathrm{C}$, and let $T_0 = 0°\mathrm{C}$, the range of actuating temperature is defined as $T_0 \leq T \leq A_f$.

In Fig. 5(b), it can be seen that three cases have the same actuating temperature of transformation since they have the same NiTi components.

4 Conclusions

The study on interface failure of SMA reinforced smart structure paves a way for an integrity evaluation of smart structures, is also a necessary link and the basis for the application of smart structures. The interface failure of SMA reinforced smart structures with damages are studied through the variational principle and the meso-mechanics method in this paper, some important conclusions are obtained:

(1) Thermo-mechanical behaviors of SMA reinforced smart structures with damages are analyzed through the shear lag model and the variational principle, mathematical expressions on the meso-displacement field, stress-strain field of a typical element with damages are obtained. Results show that the strength of smart structures can be self-adaptively controlled by SMA fibers embedded in smart structures.

(2) The criterion of interface failure for SMA reinforced smart structure with damages is established, that is, when $\tau_{i\,\max}$ is equal to the shear strength τ_b of the interface, the interface failure begins. The failure criterion is related to two kinds of actuation: dead-load and temperature, and the temperature is reflected by parameter k_2.

(3) The criterion of interface failure for SMA reinforced smart structure with damage is applied in an example.

References

1. Liberatore, S., Carman, G.P.: Damage detection of structures based on spectral methods using piezoelectric materials. Structural Health Monitoring 606–614 (2003)
2. Dolye, C., Staveley, C., Henderson, P.: Structural health monitoring using optical fibre strain sensing systems. Structural Health Monitoring 944–951 (2003)
3. Park, G., Inman, D.J., Farrar, C.R.: Recent studies in piezoelectric impedance-based structural health monitoring. Structural Health Monitoring 1423–1430 (2003)
4. Tao, B.Q.: Smart Materials and Structures. Beijing: Defense Industry Publisher (in Chinese) (1997)
5. Yasubumi, F.: Design and material evaluation of shape memory composites. Journal of Intelligent Material Systems and Structures 7(71), (1996)
6. Stalmans, R., Delaey, L., Van Humbeeck, J.: Modeling of adaptive composite materials with embedded shape memory alloy wires. Materials Research Society Symposium Proceedings **459**, 119–130 (1996)
7. Wei, Z.G., Sandstrom, R., Miyazaki, S.: Shape memory materials and hybrid composites for smart systems. Part II. Shape-memory hybrid composites. Journal of Materials Science **33** (15), 3763–3783 (1998)
8. Birman, V.: Review of mechanics of shape memory alloy structures. Applied Mechanics Review **50**(11), 629–645 (1997)
9. Boyd, G., Lagoudas, D.C.: A thermodynamical constitutive model for shape memory materials. Part II. The SMA composite material. Int. J. Plasticity **12**(7), 843–873 (1996)
10. Bo, Z., Lagoudas, D.C.: Thermomechanical modeling of polycrystalline SMAs under cyclic loading. Part I: Theoretical derivations. International Journal of Engineering Science **37**(9), 1089–1140 (1999)
11. Hu, Z.L., Xiong, K., Wang, X.W.: One-dimensional incremental constitutive relation of SMA fiber reinforced smart composites with damages. Transactions of Nanjing University of Aeronautics and Astronautics **35**(5), 465–473 (in Chinese) (2003)
12. Hu, Z.L.: Properties characterization and meso-mechanical analysis of smart structures with damages. Nanjing: [Doctor Thesis]. Nanjing University of Aeronautics and Astronautics (in Chinese) (2003)
13. Yang, Q.S.: Meso-structural Mechanics and Design of Composites. Beijing: Railroad Publisher of China (in Chinese) (2000)

14. Li, J.Y.: Finite Element Method. Beijing: Publisher of Beijing University of Posts and Telecommunications (in Chinese) (2000)
15. Hu, H.C.: Variational Principle and Application of Elasticity. Beijing: Science Press (in Chinese) (1982)
16. Xiong, K.: Study on adaptive mechanics of shape memory alloy reinforced composites. Nanjing: [Doctor Thesis]. Nanjing University of Aeronautics and Astronautics (in Chinese) (1997)

· 新材料新工艺 ·

雷达罩的综合优化设计

胡自力　　杨忠清

（南京航空航天大学无人机研究院，南京　210016）

文　摘　在分析对比现有的雷达罩设计方法基础上，针对某型直升机机载雷达罩，研究了雷达罩设计过程中的基本问题、关键技术和综合优化设计方法，运用三维射线追踪法进行了计算机辅助设计，给出了布设防雷击部件的经验公式，讨论了吸波材料选择与喷涂的基本准则。电测结果表明：加罩后的功率传输系数、反射瓣、雷达辐射特性等指标的实测数据与计算值符合较好，满足了设计要求。

关键词　雷达罩，综合优化设计，三维射线追踪技术

Integrated Optimizing Design of Radome

Hu Zili　　Yang Zhongqing

(Institute of Unmanned Aircraft, NUAA, Nanjing　210016)

Abstract　Researches on essential problems, key techniques and integrated designing methods of airborne radome in helicopter are made on basis of existing designing methods, and a computer aided design (CAD) of airborne radome is conducted by means of 3D ray tracking technique. The experiential expressions are given to lay components of preventing lightning, and selection and spraying criteria of microwave absorbing material are discussed. Electric experimental results show that measured data such as power transmission coefficient, reflection-lobes and radiation characteristic of antenna with radome are in agreement with calculated data and satisfy the design requirements.

Key words　Radome, Integrated optimizing design, 3D ray tracking technique

1　引言

世界上第一个机载雷达罩是由美国西方电气公司生产装于 B－18A 飞机上的 S 波段雷达罩[1]，它的主要功能是保护罩内雷达系统免受任何形式的损伤和破坏，同时又为该系统提供电磁明窗。雷达罩设计涉及空气动力学、电磁场理论、材料科学、结构设计及工艺技术等学科，是一项具有较大难度的系统工程。本文针对某型直升机雷达罩，从电性能、结构强度和工艺设计等方面，研究机载雷达罩的综合优化设计方法，并通过实际研制和测试进行验证。

2　电性能设计

2.1　电性能设计方法

早期的雷达罩电性能设计方法是复杂而近似

收稿日期：2004－03－19；修回日期：2004－08－09

基金项目：无人机研究院课题资助项目（6001－26004）

作者简介：胡自力，1964 年出生，博士，主要从事飞机结构设计和智能材料结构的研究工作